COMMUNICATION

Cooperativity in the Enhanced Piezoelectric Response of Polymer Nanowires

Luana Persano, Canan Dagdeviren, Claudio Maruccio, Laura De Lorenzis, and Dario Pisignano*

Piezoelectricity, a Greek term for pressure-induced electricity, is the capability of a material to polarize by means of spatially separated electrical charges of opposite sign, in response to an external stress that produces a mechanical deformation. Generally, charges accumulate at two opposite side surfaces of the material body, and, in absence of short-circuited contacts, a voltage bias is generated. This effect can be observed in materials whose crystalline state has no center of symmetry (so-called non-centrosymmetric), including polymers and biological systems.[1] To date, piezoelectricity represents one of the most valuable alternative source of energy with an associated fast-growing investment market and potential applications spanning across a wide range of fields, such as information and communications, industrial automation, healthcare and medical monitoring, defense industry, automation and robotics.[2] Indeed, the capability of harvesting energy from small mechanical forces, through pressure, vibration, bending, elongation, and compression, is today subject of extensive research on both materials and device geometries, and the related development of self-powered wireless devices could be of great importance for the internet of things, that is for interconnecting individual uniquely identifiable objects and bodies.[3,4] In this respect, piezoelectric micro- and nanostructures have demonstrated improved properties that enable new functionalities not achievable with their bulk counterpart. Most of these are related to reduced dislocations and superior mechanical properties.[5–7] For instance, in pioneering work by the Wang group, aligned arrays and multilayer stacks of zinc oxide and lead zirconate titanate nanowires have been exploited to power light-emitting and wireless devices.[8,9]

In this framework, piezoelectric polymers are very promising, since they can also provide structural flexibility and toughness, as well as low cost, improved biocompatibility, and ease of processing. In particular, the device-integration of polyvinylidene-fluoride (PVDF) and its copolymers is attracting increasing interest,[10–12] because their micro and nanostructures such as films, belts and fibers have shown unique advantages in terms of material functionality and piezoelectric response, and self-poling during nanofabrication.[13–17] Electrospinning is especially effective in this respect, producing self-poled piezoelectric nanofibers due to the very high stretching forces exerted on electrified solution jets.[17] Consequently, polymer molecules mainly align parallel to the fiber longitudinal axis,[18] and piezoelectric material phases are favored compared to films.[16,19] Furthermore, aligned arrays of PVDF-based fibers generally exhibit still superior piezoelectric performances.[20–22] Most often, these fibers are aligned with low density and provide sub-monolayer coverage of solid supports, namely they are separated by distances of the order of microns from their nearest neighbors in deposited strands. This configuration results in open-circuit currents which correspond to the sum of currents generated by each single nanowire in the generator.[23] Dense (10^7 fibers/mm²) arrays of electrospun aligned nanofibers of poly(vinylidene fluoride-*co*-trifluoroethylene) [P(VDF-TrFe)] offer exceptional piezoelectric characteristics and output voltage significantly enhanced with respect to individual fibers.[19] Such an arrangement is characterized by large sensitive areas (tens of cm²) and light weight, and it may be bent or twisted without fracture. However, the improved voltage output from aligned arrays of polymer piezoelectric nanostructures in mutual contact cannot be explained by conventional circuit theory. The in-depth understanding of this mechanism and the assessment of its possible general validity for nanofibers regardless of their constituent material or fabrication process would be very important for realizing improved mechanical energy-harvesting architectures.

Here, we provide a detailed insight into piezoelectric energy generation from arrays of polymer nanofibers. For sake of comparison, we firstly measure individual P(VDF-TrFe) fibers at well-defined levels of compressive stress. Under an applied load of 2 mN, single nanostructures generate a voltage of 0.45 mV.

Dr. L. Persano,[+] Prof. D. Pisignano
National Nanotechnology Laboratory of
Istituto Nanoscienze-CNR
Via Arnesano, I-73100, Lecce, Italy

Dr. C. Dagdeviren[+]
Department of Materials Science and Engineering
Frederick Seitz Materials Research Laboratory,
and Beckman Institute for Advanced Science
University of Illinois at Urbana-Champaign
Urbana, IL 61801, USA

Dr. C. Maruccio[+]
Dipartimento di Ingegneria dell'Innovazione
Università del Salento
Via Arnesano, I-73100, Lecce, Italy

Prof. L. De Lorenzis
Institut für Angewandte Mechanik
Technische Universität Braunschweig
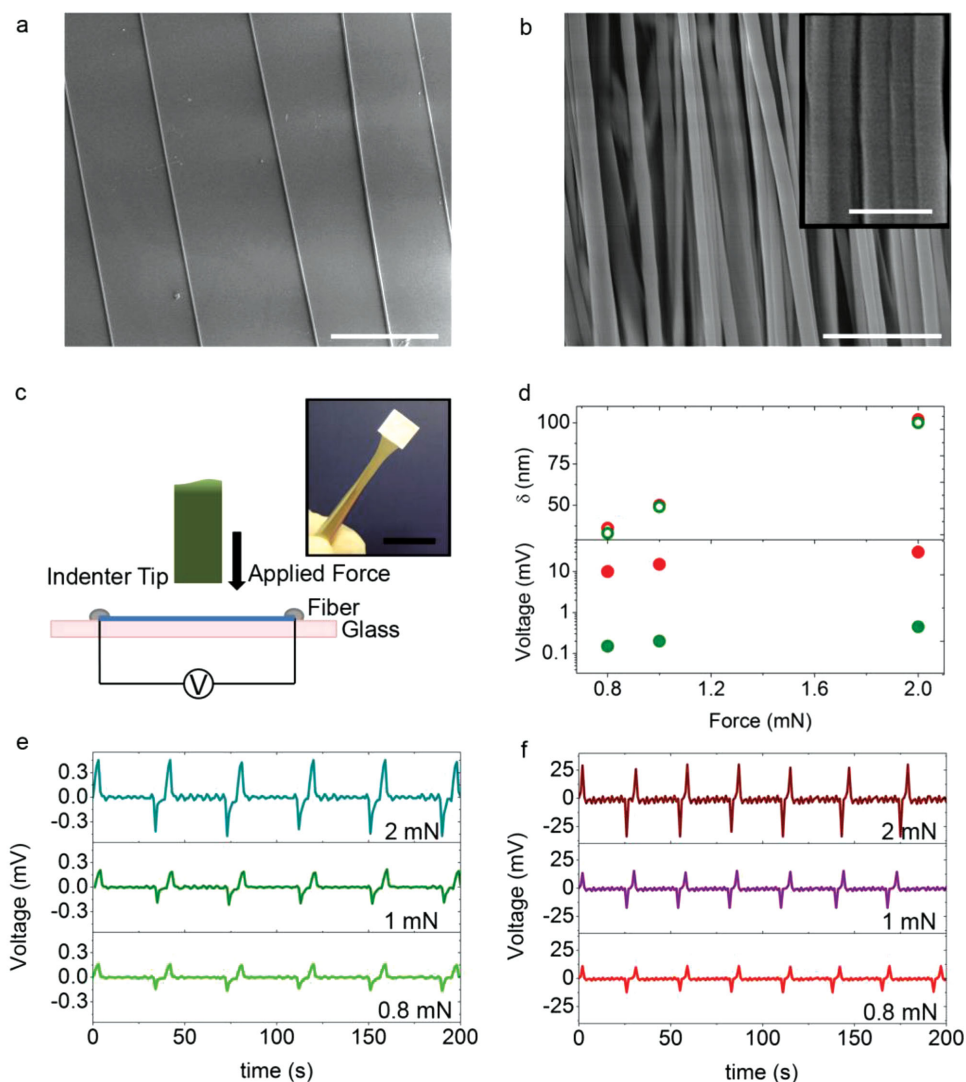Bienroder Weg 87 Campus Nord,
D-38106, Braunschweig, Germany

Prof. D. Pisignano
Dipartimento di Matematica e Fisica "Ennio De Giorgi"
Università del Salento
Via Arnesano, I-73100, Lecce, Italy
E-mail: dario.pisignano@unisalento.it

[+]These authors contributed equally to this work.

Materials
Views
www.MaterialsViews.com

ADVANCED
MATERIALS
www.advmat.de

COMMUNICATION

Figure 1. SEM images of: a) a strand of mutually isolated fibers (scale bar, 20 µm) and b) a dense array of aligned fibers at different magnification (scale bar, 3 µm). Inset: magnification of aligned fibers with line mutual contact along their side (scale bar, 1 µm). c) Schematic illustration of the experimental setup for force-indentation measurements. Inset: photograph of a fiber array sample. d) Measured displacement, δ, and voltage response of single fiber (green dots) and array of fibers (red dots) at different applied forces. e,f) Measured output voltage under repeated load/unload cycles for a single fiber (e) and an array of fibers (f). From top to bottom in (e) and (f), the applied loads are 2.0 mN, 1.0 mN and 0.8 mN, respectively.

We show that under the same load conditions, fibers in dense arrays exhibit a voltage output higher by about two orders of magnitude. Numerical modelling studies demonstrate that the enhancement of the piezoelectric response is a general phenomenon associated to the electromechanical interaction among adjacent fibers, namely a cooperative effect depending on specific geometrical parameters. This establishes new design rules for next piezoelectric nanogenerators and sensors.

P(VDF-TrFe) fibers were electrospun by a potential of 30 kV onto a collector disk with sub-cm width rotating at 4000 rpm (see Experimental Section). Strands of mutually isolated fibers were deposited onto glass coverslips, mounted on the rotating collector. Dense arrays of fibers were directly spun onto the collector surface. Representative scanning electron microscopy (SEM) images are displayed in **Figure 1**a,b. The fibers are smooth, with a uniform diameter over their

length. Array samples appear as in the photograph in the inset of Figure 1c.

To evaluate the piezoelectric response of fibers under specific compressive loads, flexible and thin Cu wires with a layer of silver epoxy were used to define contacts. For electrical measurements, both isolated fibers and arrays were positioned onto glass substrates, and a tribo-indenter TI 950 (Hysistron) equipped with a flat-ended cylinder sapphire tip (1 mm diameter) was used to apply calibrated forces. A scheme of the set-up used is reported in Figure 1c. Under applied forces of 0.8–2.0 mN, fiber displacements were in the range of 30–100 nm, related to the viscoelastic properties of the material and to the fibrous shape. No significant difference was appreciable in the displacements of individual fibers and arrays under the same applied force. A lock-in amplifier was used to collect the open-circuit voltage from the fibers when a well-defined

COMMUNICATION

level of compressive force is delivered. The data in Figure 1d highlight linear variations of the output voltage with applied force, presenting slopes of 0.2 V/N and 15 V/N for single fibers (green dots) and arrays (red dots), respectively. The piezoelectric response of P(VDF-TrFe) fibers in the arrays is strongly enhanced with respect to isolated fibers. Additional information evidencing the different response in the two systems were collected by dynamic loading-unloading cycles (Figure 1e and 1f). During compression, these measurements showed a well-behaved, periodic alternation of negative and positive peaks of the open-circuit voltage outputs, corresponding to the application and release of the stress, respectively. For identical applied loads in the range 0.8–2.0 mN, piezovoltages for isolated fibers and arrays were peaked at 0.15–0.45 mV and 10–30 mV, respectively. Hence, it is clear that dense arrays of aligned piezoelectric polymer fibers yield enhanced voltage response under identical applied forces and consequent strain conditions.

To explain in depth this behavior, we developed extensive numerical simulations through a finite element multiphysics environment, describing the complex electromechanical interaction among fibers at microscale which affects the resulting polarization measured along the direction (x_3) of the fiber length, L (**Figure 2**a). The piezoelectric polymer is described by the constitutive equations of linear piezoelasticity (see Supporting Information), and the mutual interaction of fibers is mainly due to contact between adjacent elements as a result of the applied loading. Compressive forces are applied by means of pressing plates in the direction (x_2) orthogonal to the plane defined by the array of fibers and identified by axes x_1 and x_3 as schematized in Figure 2a, and the consequent voltage distributions due to the applied pressure are then determined. For instance, the component of the electric displacement along the fiber length is

$$D_3 = \sum_{j=1}^{3} d_{3j}\sigma_{jj} + k_{33}E_3,$$ where d_{3j} are the piezoelectric coefficients, σ_{jj} are the stress components, k_{33} is the dielectric permittivity coefficient and E_3 is the electric field component in x_3 direction. The output voltage bias, V_{out}, at the two ends of fibers is then obtained directly from such analysis.

The interfiber interaction is found to have different effects depending on the stacking directions of individual nanostructures (x_1 or x_2 as shown in Figure 2b), and on the fiber cross-sectional shape. Both circular cross-sections with radius, R, well-describing our electrospun fibers, and rectangular cross-sections of width, W, and thickness, T, are considered. Fibers with rectangular cross-section are a useful basis of comparison, since modeling their stacks with zero interfiber spacing leads to describe bulk piezoelectric samples. Full details on numerical modeling are reported in the Supporting Information. In the following, we firstly analyze the behavior of single piezoelectric
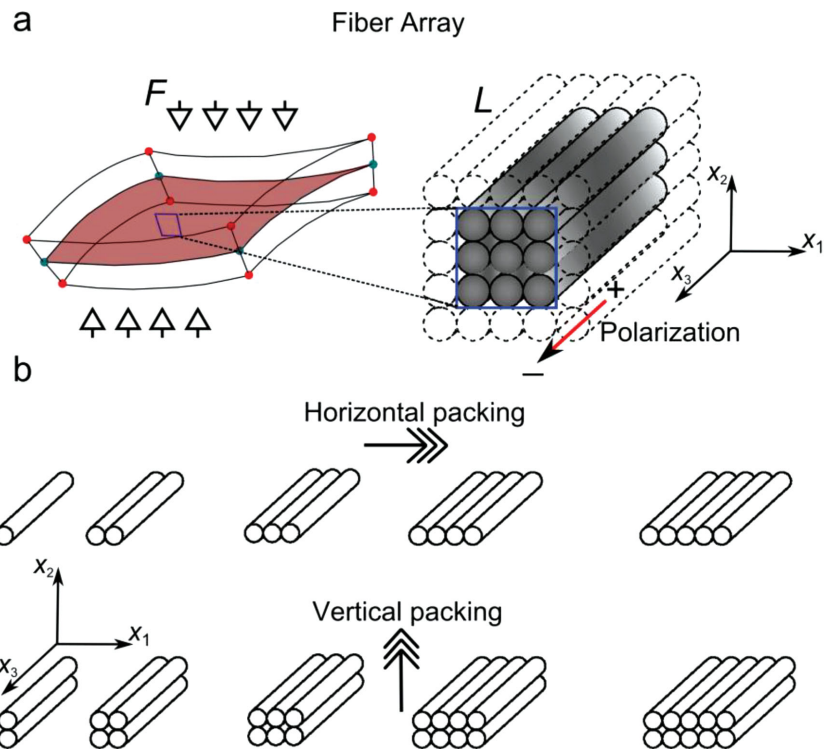

Figure 2. a) Scheme of the PVDF-based fiber array structure at macro- and micro-scale. F: applied compressive force. L: fiber length. b) Packing of fibers in the vertical and horizontal directions.

fibers, and then analyze how the output voltage is affected by the electromechanical interaction of adjacent fibers.

Single Piezoelectric Fibers: For fibers of both cylindrical and rectangular shape, increasing the length by a given factor leads to an increase of the output voltage by roughly the same factor as shown in **Figure 3**a, for same values of applied pressures. This allows the nanogenerator to be described by modeling segments of fibers much shorter than in experiments, thus significantly saving computational time. Validating such a $V_{out}(L)$ dependence, one legitimates analyzing fibers of shorter length, and using results to compute those for any desired length through linear correlation. In addition, for fibers with rectangular cross-sections we found that V_{out} does not depend on the width, W, under a constant pressure, whereas it is enhanced upon increasing the thickness, T, since the system correspondingly becomes less stiff.

A significant improvement of the piezoresponse is obtained by using cylindrical fibers. Indeed, under the same applied force, the output voltage from a cylindrical fiber is around 2.2 times that from a fiber with rectangular cross-section (Figure 3b). To further highlight the role of the cross-sectional geometry, several distortion factors are applied to the circular shape as illustrated in Figure 3c. In fact, the piezoelectric response of fibers with elliptical cross-section is enhanced upon increasing the b/a ratio, where a and b indicate the ellipse axis along the x_1 and the x_2 direction, respectively. This establishes new design rules for electrospun piezoelectric nanofibers, in which an elliptical cross-section can be obtained as a result of skin collapse following rapid solvent evaporation from the surface of electrified jets, of partial flattening when fibers impact

Materials
Views
www.MaterialsViews.com

ADVANCED
MATERIALS
www.advmat.de

COMMUNICATION
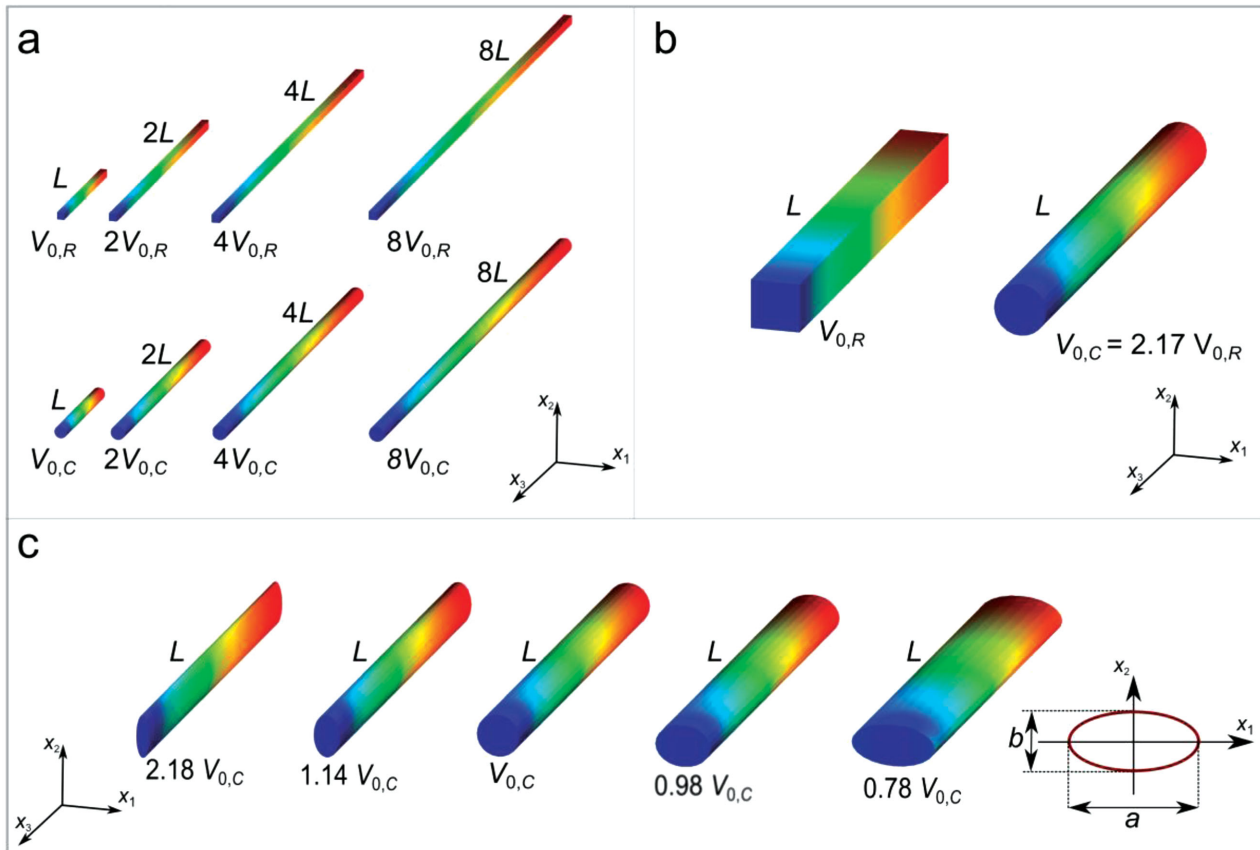
Figure 3. a) Voltage distribution on the surface of nanofibers with rectangular (*R*, top row) and circular cross-section (*C*, bottom row), and having different length (*L*, 2*L*, 4*L*, 8*L*). The same pressures (120 Pa) are applied in all the investigated cases. For each fiber, red (blue) corresponds to high (low) voltage values, and the overall output voltage bias at termination is reported, highlighting a clear proportionality between fiber length and generated voltage. $V_{0,R} = 0.90$ μV and $V_{0,C} = 1.95$ μV indicate values obtained with a fiber of length *L*. b) Comparison of nanofibers with same length, *L*, and either rectangular or circular cross-section. c) Comparison of nanofibers with elliptical cross-section and different *b/a* ratios. For each fiber, we show the corresponding output voltage which range from 2.18 to 0.78 times $V_{0,C}$ upon varying the *b/a* ratio. Bottom inset: ellipse cross-section and *a* and *b* axes.

on the collecting surface upon electrospinning with a slowly evaporating solvent component, or of both.[19,24]

Cooperative Effects in Arrays of Aligned Piezoelectric Polymer Fibers: No increase of V_{out} is found upon placing many fibers with rectangular cross-section in mutual contact and in parallel under a constant pressure, i.e., building an array along the x_1 (planar) direction which corresponds to considering a continuous, bulky piezoelectric film of thickness *T*. On the contrary, a remarkable enhancement of the piezoresponse is observed by increasing the number of adjacent cylindrical fibers along x_1. The comparison, performed for the same pressing geometry and boundary conditions, is displayed in **Figure 4**a. An increment of V_{out} up to three times is achieved by a monolayer of aligned cylindrical fibers in mutual contact compared with a film of same thickness and under the same applied pressure. Such an effect is mainly due to the electromechanical interaction among a few adjacent cylindrical fibers, giving rise to a cooperative effect in the plane of the array that restrains the transverse deformation and correspondingly increases the transverse stresses as shown in Figure 4b. This mechanism in turn leads to an increase of the piezoelectric response along the longitudinal fiber axis, and takes place when the array starts to be built. In fact, when the number of parallel fibers

in the monolayer exceeds five, no further increase of V_{out} is observed.

A more-complex cooperativity is found along the out-of-plane (x_2) direction, and obtained by stacking several layers of piezoelectric fibers. For a given value of the force applied to pressing plates and for identical pressing geometry and boundary conditions, the presence of more than a layer of fibers aligned along the vertical direction enhances the overall piezoelectric response of the system up to two orders of magnitude with respect to a monolayer, as shown in **Figure 5**a. Both the reduction of the mechanical stiffness along the thickness direction and the interfiber electromechanical contact interactions concur to such enhancement. These two effects can be assessed independently by comparing the results for the out-of-plane stacked cylindrical fibers and for a bulk system having the same total thickness. For a large number of stacked cylindrical fibers, the ratio of the output voltage to that of an equally thick piezoelectric bulk body stabilizes around a factor of two as shown in Figure 5a. These findings indicate that the thickness-related reduced stiffness of the array yields a piezoresponse enhancement which increases roughly linearly upon increasing the number of stacked layers (as for black dots in Figure 5a), whereas a further doubling of the piezoresponse is to be attributed to the electromechanical

**ADVANCED
MATERIALS**

www.advmat.de

*Materials
Views*

www.MaterialsViews.com
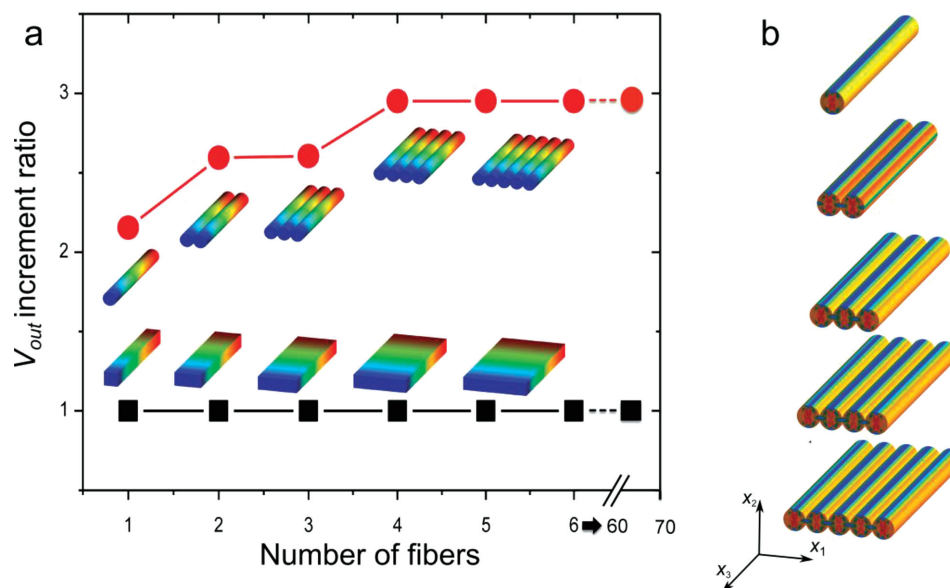
Figure 4. Cooperativity for nanofibers with different cross-sectional shape. a) Dependence of output voltage on the number of aligned fibers. Cooperativity is found only in cylindrical fibers, leading to an increment of V_{out} up to three times compared with single fibers. The insets show voltage maps. Applied pressure = 120 Pa. b) Corresponding contour levels of stress (σ_1) distribution in the nanofibers. Maximum and minimum stress values, corresponding to the used color scales (i.e., to red and blue, respectively) are, from top to bottom: +0.098 and −0.368 MPa, +0.117 and −0.489 MPa, +0.122 and −0.507 MPa, +0.156 and −0.651 MPa, +0.166 and −0.694 MPa.

contact interaction of cylindrical fibers in the array constituting the nanogenerator. The corresponding transverse stresses in the fiber arrays are displayed in Figure 5b. Through computational homogenization, we find that the cooperative behavior would correspond to the following, asymptotic effective piezoelectric coefficients: $\bar{d}_{31}$ = 19.6 pC/N, $\bar{d}_{33}$ = −29.3 pC/N, $\bar{c}_{11}$ = 1.5 GPa and $\bar{k}_{33}$ = 10.1 k_0 where k_0 is the vacuum permittivity (Supporting Information). Consequently the macroscopic effective piezoelectric voltage constants $\bar{g}_{31}$ and $\bar{g}_{33}$ would be as high as 219.7 × 10^{-3} V m N^{-1} and −329.6 × 10^{-3} V m N^{-1}, respectively.

Such description agrees well with experimental results for the different values of investigated applied forces, for both individual piezoelectric nanofibers and for their arrays, as reported in **Table 1**. Discrepancies between measured data and model predictions can be explained by considering the slight experimental dishomogeneity in fiber orientation, geometry and distribution in the array.

In summary, cooperative effects in the response of piezoelectric fibers due to electromechanical interactions on the microscale were predicted. The effect of geometry variables on the
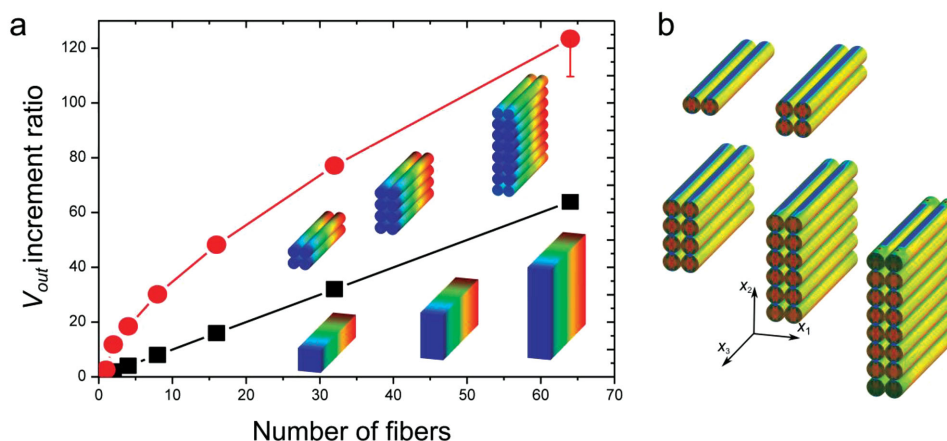
Figure 5. a) Dependence of output voltage on the number of fiber layers stacked in the x_2 direction. The overall sample thickness for 64 fibers is about 25 μm. The insets show voltage maps. Applied pressure = 120 Pa. The maximum error bar indicative of the decrease of V_{out} is estimated on the basis of the study of a possible misalignment of ±10° among fibers, as reported in the Supporting Information. b) Corresponding contour levels of stress (σ_1) distribution in the nanofibers. Maximum and minimum stress values, corresponding to the used color scales (i.e., to red and blue, respectively) are, from top-left to bottom-right: +0.117 and −0.489 MPa, +0.163 and −0.656 MPa, +0.186 and −0.730 MPa, +0.195 and −0.876 MPa, and +0.231 and −0.952 MPa.

Table 1. Comparison between experimental and numerical results.

F [mN]	Single fiber V_{out} [mV]		Array V_{out} [mV]	
	Experiment (~)	Model	Experiment (~)	Model
0.8	0.15	0.20	10	13.8
1.0	0.20	0.25	15	17.2
2.0	0.44	0.49	30	34.4

output of nanogenerators and strain sensors was investigated in detail through single-fiber experiments and parametric modeling studies, evidencing the enhancement of piezoelectric performances of cylindrical nanofibers and of their arrays compared with bulk architectures. Output piezovoltages enhanced by two orders of magnitude are achieved by arrays of uniaxially aligned fibers due to cooperative electromechanical effects. The analysis carried out in this work is of general applicability for fibers featuring linearly elastic behavior within a small deformation regime. Also, finite deformations would likely introduce quantitative but not qualitative changes to the observed effects. Examples of other piezoelectric fibers whose response can be enhanced by cooperative effects in arrays include those made of liquid crystalline polymers such as poly(γ-benzyl α-L-glutamate),[25] biomaterials like β-glycine,[26] and composites with ceramic particles.[27] A variety of fields may be envisaged, where these findings can find application during device design and realization, including vibration sensing, power sources,[28] and especially self-powered and wearable electronics,[29] smart textiles and stick-on biomedical patches for health monitoring.[30]

Experimental Section

Nanofiber Device Fabrication: P(VDF-TrFe) was purchased from Solvay Solexis and dissolved in 3:2 volume ratio of dimethylformamide (DMF)/acetone (Sigma–Aldrich). Electrospinning (ES) was performed by placing the polymer solution into a plastic syringe tipped with a 27-gauge stainless-steel needle. Voltage biases were applied to the metal needle from a high-voltage supply (EL60R0.6–22, Glassman High Voltage). During ES, the injection flow rate was kept constant at 1 mL h^{-1} with a syringe pump (Harvard Apparatus). A grounded cylindrical collector (diameter = 8 cm), was placed at a distance of 6 cm from the needle. Strands of isolated fibers were deposited onto borosilicate glass coverslips directly mounted on the rotating collector, while dense arrays of fibers were directly deposited on the surface of the collector. The produced fibers were a few centimeters long, limited by the dimensions of the glass slides used. The morphological analysis was performed by SEM with a Nova NanoSEM 450 system (FEI), using an acceleration voltage around 5 kV and an aperture size of 30 μm.

Indentation and Voltage Measurements: A tribo-indenter TI 950 (Hysistron) equipped with a flat-ended cylinder sapphire tip (1 mm diameter) was used to apply calibrated forces. A custom data-recording system consisting of a lock-in amplifier (SR830, Standard Research Systems), a multiplexer (FixYourBoard.com, U802), and a laptop was used to capture the open-circuit voltage data. Flexible, thin Cu wires with a layer of silver epoxy (Ted Pella, Inc) were used to connect the terminations of the fiber arrays. The piezoelectric measurements were carried out at room temperature.

Numerical Simulations: To numerically model the cooperative electromechanical behavior of nanostructures, a finite element multiphysics simulation environment was developed. Fibers were

discretized with linear 8-node brick elements and the interaction between individual wires is due to contact between adjacent fibers as a result of the applied loading. The implemented formulation was based on the classical master-slave concept. A detailed description of the defined model is reported in the Supporting Information.

Supporting Information

Supporting Information is available from the Wiley Online Library or from the author.

Acknowledgements

[1] A. L. Kholkin, in *Piezoelectric and Acoustic Materials for Transducer Applications*, (Eds: A. Safari, E. K. Akdoǧa), Springer, New York **2008**.

[2] L. E. Cross, W. Heywang, in *Piezoelectricity: Evolution and Future of a Technology, Springer Series in Materials Science*, (Eds: W. Heywang, K. Lubitz, W. Wersing), Springer Verlag, Berlin/Heidelberg, Germany, **2008**.

[3] Y. Zhan, Y. Mei, L. Zheng, *J. Mater. Chem. C* **2014**, *2*, 1220.

[4] C. Dagdeviren, B. D. Yang, Y. Su, P. L. Tran, P. Joe, E. Anderson, J. Xia, V. Doraiswamy, B. Dehdashtie, X. Feng, B. Lu, R. Poston, Z. Khalpey, R. Ghaffari, Y. Huang, M. J. Slepian, J. A. Rogers, *Proc. Natl. Acad. Sci. USA* **2014**, *111*, 1927.

[5] H. D. Espinosa, R. A. Bernal, M. Minary-Jolandan, *Adv. Mater.* **2012**, *24*, 4656.

[6] Z. L. Wang, W. Wu, *Angew. Chem. Int. Ed.* **2012**, *51*, 11700.

[7] S. Xu, B. J. Hansen, Z. L. Wang, *Nat. Commun* **2010**, *1*, 93.

[8] Y. F. Hu, Y. Zhang, C. Xu, L. Lin, R. L. Snyder, Z. L. Wang, *Nano Lett.* **2011**, *11*, 2572.

[9] L. Gu, N. Cui, L. Cheng, Q. Xu, Q. Bai, M. Yuan, W. Wu, J. Liu, Y. Zhao, F. Ma, Y. Qin, Z. L. Wang, *Nano Lett.* **2013**, *13*, 91.

[10] K. Asadi, D. M. de Leeuw, B. de Boer, P. W. M. Blom, *Nat. Mater.* **2008**, *7*, 547.

[11] S. H. Bae, O. Kahya, B. K. Sharma, J. Kwon, H. J. Cho, B. Ozyilmaz, J.-H. Ahn, *ACS Nano* **2013**, *7*, 3130.

[12] S. Cha, S. M. Kim, H. Kim, J. Ku, J. I. Sohn, Y. J. Park, B. J. Song, M. H. Jung, E. K. Lee, B. L. Choi, J. J. Park, Z. L. Wang, J. M. Kim, K. Kim, *Nano Lett.* **2011**, *11*, 5142.

[13] X.-Q. Fang, J.-X. Liu, V. Gupta, *Nanoscale* **2013**, *5*, 1716.

[14] C. Sun, J. Shi, D. J. Bayerl, X. Wang, **2011**, *4*, 4508.

[15] F. Fang, H. Niu, H. Wang, X. Wang, T. Lin, *Energy Environ. Sci.* **2013**, *6*, 2196.

[16] J. Fang, X. Wang, T. Lin, *J. Mater. Chem.* **2011**, *21*, 11088.

[17] C. Chang, V. H. Tran, J. Wang, Y. K. Fuh, L. Lin, *Nano Lett.* **2010**, *10*, 726.

[18] M. V. Kakade, S. Givens, K. Gardner, K. H. Lee, D. B. Chase, J. F. Rabolt, *J. Am. Chem. Soc.* **2007**, *129*, 2777.

[19] L. Persano, C. Dagdeviren, Y. Su, Y. Zhang, S. Girardo, D. Pisignano, Y. Huang, J. A. Rogers, *Nat. Commun.* **2013**, *4*, 1633.

[20] B. J. Hansen, Y. Liu, R. Yang, Z. L. Wang, *ACS Nano* **2010**, *4*, 3647.

[21] J. Pu, X. Yan, Y. Jiang, C. Chang, L. Lin, *Sens. Actuators, A* **2010**, *164*, 131.

[22] Y.-K. Fuh, S.-Y Chen, J.-C. Ye, *Appl. Phys. Lett.* **2013**, *103*, 033114.

[23] S. Xu, Y. G. Wei, J. Liu, R. Yang, Z. L. Wang, *Nano Lett.* **2008**, *8*, 4027.

[24] S. Koombhongse, W. Liu, D. H. Reneker, *J. Polym. Sci., Part B: Polym. Phys.* **2001**, *39*, 2598.

[25] D. Farrar, K. Ren, D. Cheng, S. Kim, W. Moon, W. L. Wilson, J. E. West, S. M. Yu, *Adv. Mater.* **2011**, *23*, 3954.

[26] D. Isakov, E. de Matos Gomes, I. Bdikin, B. Almeida, M. Belsley, M. Costa, V. Rodrigues, A. Heredia, *Cryst. Growth Des.* **2011**, *11*, 4288.

[27] J. Morvan, E. Buyuktanir, J. L. West, A. Jakli, *Appl. Phys. Lett.* **2012**, *100*, 063901.

[28] S. Xu, B. J. Hansen, Z. L. Wang, *Nat. Commun.* **2010**, *1*, 93.

[29] S. Xu, Y. Zhang, L. Jia, K. E. Mathewson, K.-I. Jang, J. Kim, H. Fu, X. Huang, P. Chava, R. Wang, S. Bhole, L. Wang, Y. J. Na, Y. Guan, M. Flavin, Z. Han, Y. Huang, J. A. Rogers, *Science* **2014**, *344*, 70.

[30] C. Dagdeviren, Y. Su, P. Joe, R. Yona, Y. Liu, Y.-S. Kim, Y. Huang, A. R. Damadoran, J. Xia, L. W. Martin, Y. Huang, J. A. Rogers, *Nat. Commun.* **2014**, *5*, 4496.